

TRANSFORMATION BETWEEN RATIONAL FUNCTION MODEL AND RIGOROUS SENSOR MODEL FOR HIGH RESOLUTION SATELLITE IMAGERY

S.J. Liu *, X.H. Tong

Dept. of Surveying and Geo-informatics, Tongji University, No.1239 Siping Road, Shanghai, 200092, China
liusjtj@gmail.com, tongxhtj@yeah.net

WgS-PS: WG I/5

KEY WORDS: Space Photogrammetry, High Resolution Satellite Imagery, Sensor Models, Rigorous Sensor Model, Rational Function Model, Stereo positioning, Recovery

ABSTRACT:

The rigorous sensor model based on the collinear equation describes the imaging geometric relationship between the image points and homologous ground points, with parameters which have understandable physical meanings. However, it lacks generality because of its complexity and varying with different sensor types. Especially, the physical parameters are often made unavailable intentionally or unintentionally. Rational Function Model (RFM) has been applied in remote sensing and photogrammetry to represent the transformation between the image space and object space. It attracts more attention for its generality and ability of providing almost the same accuracy as the rigorous sensor model. At the same time, there also exist some disadvantages for RFM, such as difficulty in interpreting the parameters and possibility of correlation between the RF coefficients. In order to utilize the advantages of both, this paper studied the transformation between the two models. Firstly in the experiments, RF coefficients are computed using the virtual control points generated from the rigorous sensor model. The derived RFM gives almost the same accuracy as the original model, with only 1mm decline in stereo positioning accuracy. On the other hand, as for linear array sensor images, the interior orientation (IO) parameters x_0 and f are correlated, x_0 need to be fixed as a static value in order to define a camera coordinate system for the purpose of retrieving the physical parameters. If x_0 is given, the parameters of rigorous sensor model can be retrieved with high accuracy. There is $\pm 0.001\text{mm}$ error in internal orientation parameters, $\pm 5\text{cm}$ error in perspective center coordinates and $\pm 0.002^\circ$ error in rotation angles. If x_0 is unknown and fixed as an assumed value of 0, it results in the modification of the rotation angle parameters, which compensates the departure of x_0 . The perspective center coordinates are little affected by this assumption. Further more, the retrieved rigorous sensor models of the stereo image pair are employed for geo-positioning, the accuracy decline is less than 1mm, which indicates that the proposed method for rigorous sensor model recovery is applicable.

1. INTRODUCTION

Sensor imaging model is the basis of photogrammetric processing of remote sensing images. Rigorous sensor model based on the collinear equation has described the imaging geometric relationship between the image point and the homologous ground point, with parameters which have understandable physical meanings. However, rigorous sensor model lacks generality because it is complex and varies with different sensor types. Moreover, its parameters may not be available. To solve these problems, some general imaging models have been proposed and studied, among which Rational Function Model (RFM) is most famous for its sensor independency and ability of giving almost the same accuracy as rigorous sensor model. However, RFM also has disadvantages such as difficulty in parameter interpretation and possibility of correlation between the parameters. Thus, it is necessary to study the transformation between rigorous sensor model and RFM in order to utilize the advantages of both.

There's already systematic theory about rigorous sensor model for high resolution satellite imagery. RFM has also gained widespread concern and research since the successful launch of IKONOS satellite. Dowman (2000) analyzed the accuracy and robustness of RFM and derived the algorithm for the error propagation. Yang (2000) carried out the experiments of geo-

positioning with RPCs using SPOT and NAPP images and achieved the conclusion that 3rd-order or even 2nd-order RFM with different denominators can replace rigorous sensor model for SPOT images. As for aerial images, 1st-order RFM provides sufficient accuracy. Tao (2001) specified two schemes to generate RF coefficients. One is the terrain dependent way and the other is the terrain independent way. Di (2003) investigated RFM-based positioning algorithm and accuracy improvement as well as the potential of rigorous sensor model recovery. RPC block adjustment has been discussed by Grodecki and Dial (2003). Fraser (2006) further discussed RPC block adjustment with compensation for exterior orientation biases. Li (2007) investigated the integration of IKONOS and QuickBird imagery for geo-positioning.

This paper has systematically studied the transformation between rigorous sensor model and RFM with the aim of utilizing the advantages of the two models.

2. RIGOROUS SENSOR MODEL AND RFM

2.1 Rigorous Sensor Model

According to the defined camera coordinate system in QuickBird image product, axis X is along the flight direction,

* Corresponding author

axis Y points to the left side of the detector line and axis Z points downwards. Then, the linear equation is:

$$\begin{aligned} 0 - x_0 &= f \frac{a_1(X - X_s) + b_1(Y - Y_s) + c_1(Z - Z_s)}{a_3(X - X_s) + b_3(Y - Y_s) + c_3(Z - Z_s)} = f \frac{\bar{X}}{\bar{Z}} \\ -(y - y_0) &= f \frac{a_2(X - X_s) + b_2(Y - Y_s) + c_2(Z - Z_s)}{a_3(X - X_s) + b_3(Y - Y_s) + c_3(Z - Z_s)} = f \frac{\bar{Y}}{\bar{Z}} \end{aligned} \quad (1)$$

Our objective is to retrieve the orientation parameters of the linear array sensor image from the RF coefficients. As for high resolution satellite imagery scanned by linear array sensor, each image line has its independent orientation parameters. So, strictly speaking, to recover the rigorous sensor model of a linear array sensor image, we should retrieve the orientation parameters for every image line. In view of the fact that exterior orientation (EO) parameters of the sensor are changing continuously and smoothly during image capturing, the time-varying EO parameters can be modelled by a polynomial function. If it's smooth enough, we can just use 1st-order polynomials. Generally, 2nd-order polynomials are effective to model the change (see equation 2). At the same time, the interior orientation (IO) parameters are supposed to be changeless.

$$\begin{aligned} X_{si} &= X_{s0} + X_{s1} \cdot x + X_{s2} \cdot x^2 + \dots \\ Y_{si} &= Y_{s0} + Y_{s1} \cdot x + Y_{s2} \cdot x^2 + \dots \\ Z_{si} &= Z_{s0} + Z_{s1} \cdot x + Z_{s2} \cdot x^2 + \dots \\ \varphi_i &= \varphi_0 + \varphi_1 \cdot x + \varphi_2 \cdot x^2 + \dots \\ \omega_i &= \omega_0 + \omega_1 \cdot x + \omega_2 \cdot x^2 + \dots \\ \kappa_i &= \kappa_0 + \kappa_1 \cdot x + \kappa_2 \cdot x^2 + \dots \end{aligned} \quad (2)$$

2.2 Rational Function Model

In RFM, the image plane coordinates (r, c) are described as the ratio of two polynomials whose variables are the homologous ground point's coordinates (X, Y, Z):

$$\begin{cases} r = \frac{p_1(X, Y, Z)}{p_2(X, Y, Z)} \\ c = \frac{p_3(X, Y, Z)}{p_4(X, Y, Z)} \end{cases} \quad (3)$$

Where (r, c) and (X, Y, Z) are normalized and dimensionless:

$$\begin{aligned} r &= \frac{r_{raw} - r_{offset}}{r_{scale}}, c = \frac{c_{raw} - c_{offset}}{c_{scale}} \\ X &= \frac{X_{raw} - X_{offset}}{X_{scale}}, Y = \frac{Y_{raw} - Y_{offset}}{Y_{scale}}, Z = \frac{Z_{raw} - Z_{offset}}{Z_{scale}} \end{aligned} \quad (4)$$

The normalized value is within (-1, 1). It aims to avoid the rounding error caused by the large diversity of the coordinates' magnitude to improve the computational precision. The general form of polynomial Pi (i = 1, 2, 3, 4) is:

$$P(X, Y, Z) = \sum_{i=0}^{n_1} \sum_{j=0}^{n_2} \sum_{k=0}^{n_3} c_{ijk} X^i Y^j Z^k \quad (5)$$

The polynomial coefficient c_i in equation 5 is called RPC (Rational Polynomial Coefficient). In the model, the distortion caused by optical projection can be expressed as 1st-order polynomial coefficients, and the error caused by the earth curvature, atmospheric refraction and lens distortion can be corrected by 2nd-order polynomial coefficients, and that caused by other unknown distortions can be simulated by 3rd-order polynomial coefficients. As for push-broom linear array sensors, we use the 3rd-order polynomial form.

Generally, we can use any reference system for object space coordinates in RFM. However, in view of the large ground coverage of satellite images, we usually adopt the geocentric coordinate system or the geodetic coordinate system instead of the Gauss projection system which contains projection error.

3. RPC GENERATION

Equation 3 with 3rd-order polynomials can be linearized as:

$$\begin{cases} v_r = \left(\frac{1}{D_1}, \frac{X}{D_1}, \dots, \frac{Z^3}{D_1}, -r \frac{X}{D_1}, \dots, -r \frac{Z^3}{D_1} \right) (a_0, a_1, \dots, a_{19}, b_1, \dots, b_{19})^T - \frac{r}{D_1} \\ v_c = \left(\frac{1}{D_2}, \frac{X}{D_2}, \dots, \frac{Z^3}{D_2}, -r \frac{X}{D_2}, \dots, -r \frac{Z^3}{D_2} \right) (c_0, c_1, \dots, c_{19}, d_1, \dots, d_{19})^T - \frac{c}{D_2} \end{cases} \quad (6)$$

Where

$$\begin{aligned} D_1 &= (1, X, Y, Z, \dots, X^3, Y^3, Z^3) (1, b_1, b_2, b_3, \dots, b_{17}, b_{18}, b_{19})^T \\ D_2 &= (1, X, Y, Z, \dots, X^3, Y^3, Z^3) (1, d_1, d_2, d_3, \dots, d_{17}, d_{18}, d_{19})^T \end{aligned}$$

In order to solve the RPCs, at least 39 control points (CPs) are required. The observation equation for n CPs can be expressed as:

$$V_{(2n \times 1)} = A_{(2n \times 78)} \cdot C_{(78 \times 1)} - L_{(78 \times 1)} \quad (7)$$

In computation to solve equation 7, the normal equation is sometimes ill-posed. In order to overcome this problem, a small positive number s^2 within (0, 1) can be added to the diagonal elements of the normal equation based on the Tikhonov regularization method (Neumaier, 1998) for iterative computation.

CPs used to calculate the RPCs can be generated using the known rigorous sensor model according to the terrain independent way (Tao, 2001).

4. RIGOROUS SENSOR MODEL RECOVERY

As for a frame camera image, there exists an imaging plane, the focal point is unique. However, as regards to a linear array sensor image, the image space coordinate system is not unique due to its characteristic of line imaging. The focal point can be supposed to be on the detector line or somewhere else off the line. Then the focal distance will vary with different focal point definition, that is, the focal distance is correlative with the interior parameter x_0 as illustrated in figure 1. Thus, if there's no restriction, x_0 should be fixed as a static value while calculating the parameters of the rigorous sensor model. This assumption is to define an image space coordinate system rolling the perspective center as its original point. So, theoretically, different assumptions of x_0 do not change the

perspective center's coordinates, it only results in a rotation between the user-defined coordinate system and the nominal coordinate system.

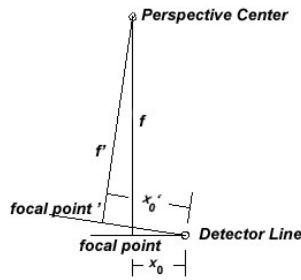


Figure 1. Illustration of focal point definition

We first generate adequate CPs along an image line using known RPCs. The orientation parameters of the line are then computed by a space resection method. Equation 1 can be linearized as:

$$\begin{cases} V_x = \frac{\partial(x)}{\partial X_s} dX_s + \frac{\partial(x)}{\partial Y_s} dY_s + \frac{\partial(x)}{\partial Z_s} dZ_s + \frac{\partial(x)}{\partial \varphi} d\varphi + \frac{\partial(x)}{\partial \omega} d\omega \\ + \frac{\partial(x)}{\partial \kappa} d\kappa + (\frac{\bar{X}}{Z})^{(i)} df - ((0-x_0) - (f \frac{\bar{X}}{Z})^{(i)}) \\ V_y = \frac{\partial(-y)}{\partial X_s} dX_s + \frac{\partial(-y)}{\partial Y_s} dY_s + \frac{\partial(-y)}{\partial Z_s} dZ_s + \frac{\partial(-y)}{\partial \varphi} d\varphi + \frac{\partial(-y)}{\partial \omega} d\omega \\ + \frac{\partial(-y)}{\partial \kappa} d\kappa - dy_0 + (\frac{\bar{Y}}{Z})^{(i)} df - (-(y-y_0) - (f \frac{\bar{Y}}{Z})^{(i)}) \end{cases} \quad (8)$$

Initially, the orientation parameters of two image lines at the beginning and the end of the image scene can be retrieved by the space resection method according to equation 8. Then we can use them to estimate the approximate values of the coefficients of the constant and 1st-order terms of the EO polynomials, and the coefficients of the 2nd-order terms are initially set to zero. Subsequently, the initial values of the IO parameters and EO polynomial coefficients together with all the CPs can be employed to build adjustment equations (see equation 9) to calculate the parameters of the rigorous sensor model.

$$\begin{bmatrix} v_{x_1} \\ \vdots \\ v_{x_n} \\ \vdots \\ v_{y_1} \\ \vdots \\ v_{y_n} \end{bmatrix} = \begin{bmatrix} \frac{\partial(-x_1)}{\partial X_{s0}} & \dots & \frac{\partial(-x_1)}{\partial X_{s1}} & x_1 \frac{\partial(-x_1)}{\partial X_{s1}} & \dots & x_1 \frac{\partial(-x_1)}{\partial X_{s2}} & \dots & x_1 \frac{\partial(-x_1)}{\partial X_{s2}} & \dots & \frac{\partial(-x_1)}{\partial \varphi} & 0 & \dots \\ \frac{\partial(-x_1)}{\partial X_{s0}} & \dots & \frac{\partial(-x_1)}{\partial X_{s1}} & x_1 \frac{\partial(-x_1)}{\partial X_{s1}} & \dots & x_1 \frac{\partial(-x_1)}{\partial X_{s2}} & \dots & x_1 \frac{\partial(-x_1)}{\partial X_{s2}} & \dots & 0 & \frac{\partial(-x_1)}{\partial \omega} & \dots \\ \vdots & \vdots & \vdots & \vdots & \vdots & \vdots & \vdots & \vdots & \vdots & \vdots & \vdots & \vdots \\ \frac{\partial(-x_n)}{\partial X_{s0}} & \dots & \frac{\partial(-x_n)}{\partial X_{s1}} & x_n \frac{\partial(-x_n)}{\partial X_{s1}} & \dots & x_n \frac{\partial(-x_n)}{\partial X_{s2}} & \dots & x_n \frac{\partial(-x_n)}{\partial X_{s2}} & \dots & \frac{\partial(-x_n)}{\partial \varphi} & 0 & \dots \\ \frac{\partial(-x_n)}{\partial X_{s0}} & \dots & \frac{\partial(-x_n)}{\partial X_{s1}} & x_n \frac{\partial(-x_n)}{\partial X_{s1}} & \dots & x_n \frac{\partial(-x_n)}{\partial X_{s2}} & \dots & x_n \frac{\partial(-x_n)}{\partial X_{s2}} & \dots & 0 & \frac{\partial(-x_n)}{\partial \omega} & \dots \\ \vdots & \vdots & \vdots & \vdots & \vdots & \vdots & \vdots & \vdots & \vdots & \vdots & \vdots & \vdots \\ \frac{\partial(-y_1)}{\partial X_{s0}} & \dots & \frac{\partial(-y_1)}{\partial X_{s1}} & x_1 \frac{\partial(-y_1)}{\partial X_{s1}} & \dots & x_1 \frac{\partial(-y_1)}{\partial X_{s2}} & \dots & x_1 \frac{\partial(-y_1)}{\partial X_{s2}} & \dots & 0 & \frac{\partial(-y_1)}{\partial \omega} & \dots \\ \vdots & \vdots & \vdots & \vdots & \vdots & \vdots & \vdots & \vdots & \vdots & \vdots & \vdots & \vdots \\ \frac{\partial(-y_n)}{\partial X_{s0}} & \dots & \frac{\partial(-y_n)}{\partial X_{s1}} & x_n \frac{\partial(-y_n)}{\partial X_{s1}} & \dots & x_n \frac{\partial(-y_n)}{\partial X_{s2}} & \dots & x_n \frac{\partial(-y_n)}{\partial X_{s2}} & \dots & 0 & \frac{\partial(-y_n)}{\partial \omega} & \dots \\ \vdots & \vdots & \vdots & \vdots & \vdots & \vdots & \vdots & \vdots & \vdots & \vdots & \vdots & \vdots \end{bmatrix} \begin{bmatrix} dX_{s0} \\ dk_0 \\ dX_{s1} \\ dk_1 \\ dX_{s2} \\ dk_2 \\ dk_2 \\ df \\ dy_0 \end{bmatrix} + \begin{bmatrix} -(0-x_0) - (f \frac{\bar{X}_1}{Z})^{(i)} \\ (y_1 - y_0^{(i)}) - (f \frac{\bar{Y}_1}{Z})^{(i)} \\ \vdots \\ -(0-x_0) - (f \frac{\bar{X}_n}{Z})^{(i)} \\ (y_n - y_0^{(i)}) - (f \frac{\bar{Y}_n}{Z})^{(i)} \end{bmatrix} \quad (9)$$

5. EXPERIMENTS

5.1 RPCs Generation

The images used in the experiments are QuickBird separate-orbit stereo image pair in Shanghai district, China (see Figure 2), acquired in Feb. 2004 and May 2004, with size of 27,552 pixels × 25,776 pixels and 27,552 pixels × 25,952 pixels, which is about 16 km × 16km on the ground. The original data of the sensor and orbit can be read from the image support data (ISD) to calculate the parameters of rigorous sensor model with 2nd-order EO polynomials. Table 1 lists the parameters of the rigorous sensor mode of the left image. Then, 1000 virtual CPs and 1000 check points distributed in 10 elevation layers ranging from -1000m to 1000m are generated in the object space using the rigorous sensor models of the stereo image pair. The virtual CPs are used to generate the RPCs, and the check points are used to estimate the application accuracy of stereo positioning using the derived RPCs. Table 2 shows the residuals of RPCs generation, and the stereo positioning accuracy using the derived RPCs of the stereo image pair is illustrated in table 3.



Figure 2. QuickBird stereo image pair in Shanghai district, China

	constant	1 st -order	2 nd -order
X_s	-2988209.7102	-782.846146	2.18145551
Y_s	4902864.8851	4313.671710	-3.01160415
Z_s	3683427.0321	-6355.128372	-2.31027491
φ	-2.8028355171	0.0005318117	0.0000078574
ω	0.5515148505	0.0062452430	0.0000477436
κ	0.9465309385	-0.0002106895	-0.0000112659
Detpitch = 0.01191396mm/pixel			
$f = 8836.202\text{mm} = 741667.928 \text{ pixel}$			
$x_0 = 9.54684\text{mm} = 801.315 \text{ pixel}$			
$y_0 = 164.02773\text{mm} = 13767.692 \text{ pixel}$			

Table 1. Parameters of rigorous sensor model of the left Quickbird image

	Left image		Right image	
	line	sample	line	sample
Max	0.00064	0.00044	0.00028	0.00214
RMSE	0.00035	0.00022	0.00009	0.00112

Table 2. Residuals of RPCs generation of the stereo images (units: pixel)

	$ \Delta X $	$ \Delta Y $	$ \Delta Z $
Max	0.0025	0.0019	0.0024
RMSE	0.0008	0.0009	0.0011

Table 3. Stereo positioning accuracy using the derived RPCs (units: meter)

From table 2 and table 3 we can see that RFM provides almost the equal accuracy as rigorous sensor model not only in the image space, but also in the object space for geo-positioning application, which is in agreement with other published research results.

5.2 Rigorous Sensor Model Recovery

In the above section, we have obtained the RPCs of the stereo image pair. We use them to generate 3000 virtual CPs distributed in 10 elevation layers ranging from -1000m to 1000m. The way we generate virtual CPs here, is different from that in the above section. That is, the grid we first defined in this section is in the image plane, with 30 columns multiplying 100 rows. Then we transformed the 2D grid points in the image plane to 3000 3D grid points in the object space using the RPCs and the 10 elevation layers. Table 4 lists the physical parameters retrieved from RPCs with assumption that x_0 is given, and table 5 lists the results obtained by fixing x_0 as the assumed value of 0. In the bracket is the deviation compared with the true value listed in table 1.

	constant	1 st -order	2 nd -order
X_s	-2988209.7234 (-0.0132m)	-782.848173	2.18155621
Y_s	4902864.9149 (0.0299m)	4313.672649	-3.01196493
Z_s	3683427.0781 (0.0460m)	-6355.129746	-2.31002792
φ	-2.8028355200 (-0.000598'')	0.0005318174	0.00000392
ω	0.5515148495 (-0.000206'')	0.0062452446	0.0000238709
κ	0.9465309395 (0.000206'')	-0.0002106919	-0.0000056329
$f=741668.012$ pixel (0.001001mm)			
$x_0 \equiv 801.315$ pixel			
$y_0 = 13767.689$ pixel (-0.000036mm)			
Residuals		line	sample
Max		0.00042	0.00099
RMSE		0.00020	0.00060

Table 4. Retrieved parameters of rigorous sensor model (assuming x_0 is given)

	constant	1 st -order	2 nd -order
X_s	-2988209.7739 (-0.0638m)	-782.762970	2.15844163
Y_s	4902864.9202 (0.0352m)	4313.657097	-3.00738126
Z_s	3683427.0503 (0.01822m)	-6355.092264	-2.32042619
φ	-2.8035764130 (-153.043162'')	0.0005285350	0.0000039453
ω	0.5506380923	0.0062453408	0.0000238849

κ	(-181.107558'')	0.9469188775 (80.134620'')	-0.0002050352	-0.0000056161
$f=741668.435$ pixel (0.006068mm)				
$x_0 \equiv 0$ pixel				
$y_0 = 13767.681$ pixel (-0.000129mm)				
Residuals		line	sample	
Max		0.00045	0.00102	
RMSE		0.00021	0.00059	

Table 5. Retrieved parameters of rigorous sensor model (assuming x_0 equals 0)

The residuals in the two cases are less than 0.001pixel, which indicates that model precisions in the two cases are both very high. If x_0 is given, the parameters of rigorous sensor model can be retrieved with high accuracy. There is ± 0.001 mm error in internal orientation parameters, ± 5 cm error in perspective center coordinates and $\pm 0.002''$ error in rotation angles. If x_0 is unknown and set to 0, it results in the modification of the angle parameters to compensate the departure of x_0 . The position parameters and y_0 , however, are little affected.

Next objective is to estimate the application accuracy of geo-positioning using the recovered physical parameters of the stereo images. With 1000 check points generated by RRCs, we get the statistic results listed in table 6. It shows that accuracy decline is less than 0.001m and, what's more, different assumption of x_0 does not affect the stereo positioning accuracy.

	x_0 is given			x_0 is set to 0		
	$ \Delta X $	$ \Delta Y $	$ \Delta Z $	$ \Delta X $	$ \Delta Y $	$ \Delta Z $
Max	0.0004	0.0001	0.0008	0.0004	0.0006	0.0008
RMSE	0.0002	0.0000	0.0003	0.0001	0.0002	0.0003

Table 6. Stereo positioning accuracy using the recovered physical parameters (units: meter)

6. CONCLUSION

According to the investigation and experiments, we can implement the transformation between rigorous sensor model and RFM with necessary assumption. RFM derived from rigorous sensor model provides almost the same accuracy as the latter, with only 1mm decline in stereo positioning accuracy. It is in agreement with other published research results. As for linear array sensor images, the IO parameters x_0 and f are correlated, so x_0 need to be fixed as a static value in order to retrieve the physical parameters. If x_0 is given, the physical parameters can be retrieved with high accuracy. This assumption for x_0 only causes a small rotation between the user-defined camera coordinate system and the real camera coordinate system, the perspective center coordinates and the stereo positioning accuracy won't not affected, which is proved in the experiments. Further more, using the retrieved rigorous sensor models of the stereo images for geo-positioning, the accuracy decline is less than 1mm. It indicates that the proposed method for rigorous sensor model recovery is applicable.

REFERENCE

- Yang, X.H., 2000. Accuracy of rational function approximation in photogrammetry. *ASPRS 2000 Annual Conference Proceeding*, Washington D.C., USA, pp. 23-27.
- Neumaier, A., 1998. Solving Ill-conditioned and Singular Linear System: A Tutorial on Regularization, *SIAM Review*, 40(3), pp.636-666.
- Fraser, C.S. and Hanley, H.B., 2003. Bias compensation in rational functions for Ikonos satellite imagery. *Photogrammetric Engineering and Remote Sensing*, 69(1), pp.53-58.
- Fraser, C.S. and Hanley, H.B., 2005. Bias compensated RPCs for sensor orientation of high-resolution satellite imagery. *Photogrammetric Engineering and Remote Sensing*, 71(8), pp.909-915.
- Fraser, C.S., Dial, G. and Grodecki J., 2006. Sensor orientation via RPCs. *ISPRS*, v60, n3, 182-194(2006).
http://www.geoict.net/Resources/Publications/IAPRS2004_RF_M2394.pdf
- Dowman I. and Dolloff J.T., 2000. An Evaluation of Rational Functions for Photogrammetric Restitution. *International Archives of Photogrammetry and Remote Sensing*, Amsterdam, XXXIII (B3).
- Di K., Ma R. and Li R., 2003. Rational functions and potential for rigorous sensor model recovery. *Photogrammetric Engineering and Remote Sensing*, 69(1), pp. 33-41.
- Li R., Di K. and Ma R., 2003. 3-D shoreline extraction from IKONOS satellite imagery. *The 4th Special Issue on C&MGIS, Journal of Marine Geodesy*, 26(1/2), pp.107-115.
- Wang J., Di K., Ma R., and Li R., 2005. Evaluation and Improvement of Geo-positioning Accuracy of IKONOS Stereo Imagery. *ASCE Journal of Surveying Engineering*, 131(2), pp.35-42.
- Li R., Zhou F., Niu X. and Di K., 2007. Integration of IKONOS and QuickBird Imagery for Geopositioning Accuracy Analysis. *Photogrammetric Engineering and Remote Sensing*, 73(9), pp.1067-1074.
- Grodecki, J. and Dial, G., 2003. Block adjustment of high-resolution satellite images described by rational polynomials. *Photogrammetric Engineering and Remote Sensing*, 69(1), pp.59-68.
- Tao C.V. and Hu Y., 2001. A comprehensive study of the rational function model for photogrammetric processing. *Photogrammetric Engineering and Remote Sensing*, 67(12), pp.1347-1357.
- Jacobsen K., 2006. Pros and cons of the orientation of very high resolution optical space images, *Revue Francaise de Photogrammetrie et de Teledetection*, pp.41-47.
- Habib A., Sung W.S, Kim K., Kim C., Bang K.I., Kim E.M. and Lee D.C., 2007. Comprehensive analysis of sensor modeling alternatives for high resolution imaging satellites. *Photogrammetric Engineering and Remote Sensing*, v73, n11, pp.1241-1251.
- Toutin T., 2006. Comparison of 3D physical and empirical models for generating DSMs from stereo HR images. *Photogrammetric Engineering and Remote Sensing*, v72, n5, pp.597-604.
- QuickBird Imagery Products - Product Guide, *Digital Globe, Inc.*, 2006.

ACKNOWLEDGEMENTS

The work described in this paper was substantially supported by the National Natural Science Foundation of China (Project No. 40771174), the 863 Project (Project No. 2007AA12Z178), the Program for New Century Excellent Talents in Universities (Project No. NCET-06-0381), the Foundation of Shanghai ShuGuang Scholarship Program (Project No. 07SG24), and the grants from the Doctoral Program of Higher Education of China (Project No. 20070247046). The authors thank Dr. Ronxing Li for his valuable comments on the paper.

